




Dependence of COVID-19 Policies on End-of-Year Holiday Contacts in Mexico City Metropolitan Area: A Modeling Study

Fernando Alarid-Escudero , Valeria Gracia, Andrea Luviano , Jorge Roa, Yadira Peralta, Marissa B. Reitsma, Anneke L. Claypool , Joshua A. Salomon, David M. Studdert, Jason R. Andrews, Jeremy D. Goldhaber-Fiebert, and Stanford-CIDE Coronavirus Simulation Model (SC-COSMO) Modeling Consortium

Abstract

Background. Mexico City Metropolitan Area (MCMA) has the largest number of COVID-19 (coronavirus disease 2019) cases in Mexico and is at risk of exceeding its hospital capacity in early 2021. **Methods.** We used the Stanford-CIDE Coronavirus Simulation Model (SC-COSMO), a dynamic transmission model of COVID-19, to evaluate the effect of policies considering increased contacts during the end-of-year holidays, intensification of physical distancing, and school reopening on projected confirmed cases and deaths, hospital demand, and hospital capacity exceedance. Model parameters were derived from primary data, literature, and calibrated. **Results.** Following high levels of holiday contacts even with no in-person schooling, MCMA will have 0.9 million (95% prediction interval 0.3–1.6) additional COVID-19 cases between December 7, 2020, and March 7, 2021, and hospitalizations will peak at 26,000 (8,300–54,500) on January 25, 2021, with a 97% chance of exceeding COVID-19-specific capacity (9,667 beds). If MCMA were to control holiday contacts, the city could reopen in-person schools, provided they increase physical distancing with 0.5 million (0.2–0.9) additional cases and hospitalizations peaking at 12,000 (3,700–27,000) on January 19, 2021 (60% chance of exceedance). **Conclusion.** MCMA must increase COVID-19 hospital capacity under all scenarios considered. MCMA's ability to reopen schools in early 2021 depends on sustaining physical distancing and on controlling contacts during the end-of-year holiday.

Keywords

COVID-19, dynamic transmission model, hospital capacity, Mexico, non-pharmaceutical interventions

Date received: March 1, 2021; accepted: August 28, 2021

Background

The COVID-19 (coronavirus disease 2019) global pandemic reached an estimated 72.9 million confirmed cases and caused 1.6 million deaths by December 17, 2020, with recent incidence rising sharply in low- and middle-income countries (LMICs), especially in Latin America.¹ Older individuals and those with comorbidities face greater risks of severe health outcomes and death.² Appropriate and timely hospitalization and in-hospital care can mitigate negative health outcomes.³ However,

even in highly developed countries, rapidly rising cases have overwhelmed health systems, reducing their effectiveness.⁴ Hence, governments in LMICs, like Mexico, are deeply concerned about how their less well-resourced

Corresponding Author

Fernando Alarid-Escudero, Division of Public Administration, Center for Research and Teaching in Economics (CIDE), Circuito Tecnopol Norte 117, Col. Tecnopol Pocitos II, Aguascalientes, Aguascalientes 20313, Mexico; Telephone: + 52 (449) 994 51505238 (fernando.alarid@cide.edu).



health care systems will cope with surges in COVID-19 cases.

In mid-December, Mexico had the 12th highest number of confirmed COVID-19 cases worldwide and the second-largest number of COVID-19 deaths in Latin America.¹ Mexico's crude case fatality ratio (CFR)—9.1%—is the second-highest in the world.⁵ With a population of more than 20 million residents, Mexico City Metropolitan Area (MCMA) has the highest number and incidence rate of confirmed COVID-19 cases in Mexico and a crude CFR of 8.1%.⁶ This relatively high crude CFR is likely due in part to a low testing capacity; Mexico's testing rate is one of the lowest in the world.⁷

In the coming months, non-pharmaceutical interventions (NPIs) will remain the primary means of controlling the COVID-19 epidemic in LMICs, even as vaccines are scaled up globally.⁸ However, because NPIs, especially business and school closures, can be highly disruptive to economic and social well-being, particularly in settings where many households lack computers and an internet connection,⁹ their strictness must be balanced against threats to a functioning health care system. Traditional end-of-year holiday festivities, in which many people gather and mix, present particular challenges for Mexico.¹⁰

To inform Mexico's decision makers given transmission risks posed by increased end-of-year holiday contacts and the possible health and health care impacts of

epidemic growth in early 2021, we provide model-based assessments of policy alternatives. The assessments are informed by primary data analyses. In addition to epidemic outcomes, we focus on estimating the risk that MCMA's hospital system will be saturated by early 2021 and the potential for policies and hospital capacity expansion to mitigate this.

Methods

Overview

We implemented a model of MCMA's COVID-19 epidemic and potential interventions using the SC-COSMO (Stanford-CIDE Coronavirus Simulation Model) framework (Supplemental Material). We parameterized the model based on the best available clinical and epidemiological data from published and publicly available pre-published studies, along with primary data on MCMA's hospitalization and testing infrastructure. We calibrated the model to time-series data on MCMA's daily confirmed COVID-19 cases and estimated mortality parameters by fitting Cox survival models with penalized smoothing splines to deaths and hospital occupancy from February 24, 2020, to December 7, 2020. We estimated the average time spent hospitalized from data on hospital occupancy during the same period. Model calibration determined the joint posterior uncertainty distribution of inputs. The calibrated model projected epidemic and health systems outcomes and their uncertainty under a range of intervention scenarios from December 7, 2020, to March 7, 2021. Scenarios comprised varying combinations of increased contacts during the end-of-year holiday season, followed by intensifying NPIs and reopening schools.

Model Structure and Assumptions

SC-COSMO is an age-structured, multicompartment susceptible-exposed-infected-recovered (AS-MC-SEIR) model of SARS-CoV-2 transmission and progression (Supplementary Figure S8) with realistic demography and contact patterns (household and venue-specific, non-household contacts) enabling finer detail of the interventions considered.¹¹ Specifically, SC-COSMO comprises a community transmission model and a household submodel that tracks the proportion of households whose members are in various disease states of COVID-19's natural history. SC-COSMO includes both latency and incubation, whose durations are assumed to be gamma-distributed. It incorporates the timing of NPIs (e.g., "physical distancing") and reductions of effective contacts, which may differ by age and venue. Forward

Division of Public Administration, Center for Research and Teaching in Economics (CIDE), Aguascalientes, Mexico (FAE); Center for Research and Teaching in Economics (CIDE), Aguascalientes, Mexico (VG, AL, JR); Division of Economics, Center for Research and Teaching in Economics (CIDE), Aguascalientes, Mexico (YP); Center for Health Policy and the Center for Primary Care and Outcomes Research, Department of Health Policy and The Freeman Spogli Institute, Stanford University, Stanford, California (MBR, JAS, JDGF); Department of Management Science and Engineering, Stanford University, Stanford, California (ALC); Stanford Law School and Stanford Health Policy, Stanford University, Stanford, California (DMS); Division of Infectious Diseases and Geographic Medicine, Stanford University School of Medicine, Stanford, California (JRA). The author(s) declared no potential conflicts of interest with respect to the research, authorship, and/or publication of this article. The author(s) disclosed receipt of the following financial support for the research, authorship, and/or publication of this article: Financial support for this study was provided in parts by a grant from the Society for Medical Decision Making (SMDM) funded by the Gordon and Betty Moore Foundation, a grant from Open Society Foundations (OSF), a research support fund from CIDE (FAI 0920-1424), a gift from the Wadhvani Institute for Artificial Intelligence Foundation, and Advanced Micro Devices (Santa Clara, CA, USA) provided a donation of servers. The funding agreement ensured the authors' independence in designing the study, interpreting the data, writing, and publishing the report.

Table 1 Demographic, Health System Capacity, and COVID-19 (Coronavirus Disease 2019) Outcome Data for Mexico City Metropolitan Area (MCMA)

	Value	Source
Demography		
Total population in the state of MCMA	21,942,666	CONAPO ¹⁴
Population density (population/mi ²)	53,339	CONAPO ¹⁴ and INEGI ³¹
Health system COVID-19 capacity as of December 7, 2020		
Total hospital beds	9,667	Digital Agency for Public Innovation ¹⁵
Beds with ventilators	2,659	Digital Agency for Public Innovation ¹⁵
COVID-19 outcomes as of December 7, 2020		
Cases	344,028	Ministry of Health of Mexico ⁶
Cumulative case rate (per 100,000)	1,568	Author's calculation
Deaths	28,077	Ministry of Health of Mexico ⁶
Cumulative death rate (per 100,000)	128	Authors' calculation
Hospitalized patients	68,225	Ministry of Health of Mexico ⁶
Hospitalized patients requiring ventilator	12,458	Ministry of Health of Mexico ⁶

projections with the SC-COSMO model can compare future scenarios and consider various outcomes (e.g., infections, cases, deaths, hospitalizations). The model is implemented in the R programming language.¹² We provide an R package (<https://github.com/SC-COSMO/scosmomcma>) that includes all the code to replicate the analyses and results reported in this article. The version of the package released in this article is available at <https://zenodo.org/badge/latest/doi/371769010>. A detailed description of SC-COSMO is included in the Supplemental Material.

Scenarios and Policies

We used the model to evaluate a range of policies under two scenarios involving heightened levels of social contacts in MCMA during the end-of-year holiday period (December 24, 2020, through January 6, 2021) relative to the level of preholiday social contacts on December 7, 2020, which is estimated through model calibration. Compared with the calibrated level of reductions in physical distancing on December 7, our base case scenario assumes that with less compliance with NPIs, reductions in holiday contacts will be less effective. Specifically, we increased by 51% the preholiday non-household and non-school contacts estimated for December 7 through model calibration. In an alternative scenario, we assume that December 7 contact levels are unchanged under the end-of-year holiday period.

Under each holiday contact scenario, we considered the effect of four different disease control policies followed during the period from December 7, 2020, to March 7, 2021. Policies involved increased compliance with physical distancing in the community and in-person

school reopening. They included the following: 1) status quo in which physical distancing estimated for December 7 again resumes after the holidays with schools remaining closed; 2) increased compliance with community physical distancing on January 11, 2021, with schools remaining closed; 3) status quo community physical distancing with schools reopening on January 11, 2021, with status quo in-school contacts; and 4) increased compliance with community physical distancing with schools reopening both on January 11, 2021, with reduced in-school contacts.

Outcomes

Our primary outcomes were time series of incident and cumulative COVID-19 cases, deaths, and hospitalization demand relative to MCMA hospital capacity. We estimated the effective reproduction number, R_e , for March 23, 2020—the day Mexico implemented national-level NPIs—as well as for all days since then.¹³ We also estimated the probability of hospitalization demand exceeding COVID-19-specific capacity over time.

Data and Model Inputs

MCMA consists of Mexico City's counties plus 60 counties of two neighboring Mexican states (Supplementary Figure S1). The list of counties that form MCMA and their projected 2020 population is shown in Supplementary Table S1. Overall demographic data on MCMA, including its age structure and age-specific background mortality rates, were derived from official statistics (Table 1).¹⁴ We collapsed ages into eight groups that reflected likely exposure patterns (e.g., school-age children, retirees, etc.).

We compiled publicly available data from Mexico's Ministry of Health on all detected cases and deaths in MCMA from February 24 through December 7, 2020.⁶ We used these data to compute daily incident and cumulative confirmed cases and deaths and estimate time-varying case fatality rates with proportional hazard models that included penalized smoothing splines on calendar time. We also implemented time-varying effects of MCMA's previously implemented NPIs (e.g., lockdown, physical distancing, masking, etc.) expressed as a proportionate reduction of pre-epidemic levels of effective daily contacts by segmented periods. We estimated the time points at which there was a structural change (change-points) in the levels of mobility as a proxy of changes in physical contacts (Supplemental Material). Specifically, we fitted piecewise linear models to Google's mobility data by treating the percentage difference in mobility compared to pre-epidemic levels as a random variable and estimated a varying number of changepoints.

We received daily updates from MCMA's Digital Agency for Public Innovation¹⁵ on hospital inpatient census of severe-acute respiratory infection (SARI) beds with and without ventilator occupancy, as well as current hospital capacity, which has expanded over time. We estimated time-varying hospital length of stay for COVID-19 patients, stratified by whether they required a ventilator via model calibration.

Literature reviews provided COVID-19-specific epidemiologic parameters. Latent and incubation periods were assumed to follow a gamma distribution (Supplemental Material).¹⁶⁻¹⁸ Notably, the probability of hospitalization and death among cases is not derived from the literature; they are estimated from the primary data, as described above.

Model Calibration and Uncertainty Analysis

We used Bayesian methods to calibrate 11 model parameters that could not be directly estimated from data. The parameters concerned transmission in the community and the household, time-varying case detection rates, and time-varying effects of MCMA's previously implemented NPIs (Supplemental Material). Calibration inferred values for model parameters by matching modeled outcomes to daily incident confirmed COVID-19 cases (i.e., calibration targets) from February 24 to December 7, 2020. Comparison of modeled outcomes and empirical data used a likelihood function, which we constructed by assuming that targets follow negative binomial distributions with means given by the model-predicted outputs and a dispersion equal to one, to

account for potential overdispersion in the target data.¹⁹ We defined uniform prior distributions for all calibrated parameters with ranges based on existing evidence, epidemic theory, and plausibility (Table 2). Calibration resulted in an estimate of the joint posterior uncertainty distribution for the model parameters.

To conduct the Bayesian calibration, we used the incremental mixture importance sampling (IMIS) algorithm,²⁰ which has been previously used to calibrate health policy models.^{21,22} Briefly, we sampled 10,000 parameter sets from our priors in the first stage, followed by 1,000 samples in each of the consecutive 55 updated sampling stages. This procedure yielded a posterior distribution from which we obtained 1,000 samples used for our projections and analyses. The marginal posterior distributions and pairwise comparisons are shown in Supplementary Figures S2 and S3.

We accounted for model input parameter uncertainty for all outcome measures by randomly sampling from the joint posterior distribution obtained from the Bayesian calibration. We used 1,000 parameter sets sampled from the posterior distribution to generate all primary outcomes for all scenarios and policies with 95% posterior model-prediction intervals (PI) for each outcome from the 2.5th and 97.5th percentiles of the projected values.

Sensitivity Analysis

Children may face lower transmissibility, risk of hospitalization, and mortality than the older population.²³⁻²⁵ To analyze the effects of these differential dynamics in children younger than 15 years old, we conducted a sensitivity analysis reducing children's susceptibility by 75%,²³ their mortality risk by 94%, their risk of hospitalization by 64%, and their risk of hospitalizations requiring ventilator by 37%, which were derived from observed data. We recalibrated the model under these assumptions, simulated all the scenarios and policies described above, and compared the results as differences in outcomes between the base-case and this sensitivity analysis during the projection period.

Results

MCMA's Epidemic to Date

The COVID-19 epidemic in MCMA has involved substantial burdens of cases, hospitalizations, and deaths, which the SC-COSMO model replicates (Figures 1 and 2). Case rates rose from mid-March through late May, remained high through mid-October, and have steadily increased since then (Figure 1). Trends in deaths and

Table 2 Model Input Parameters

Calibrated Parameters				
Parameter	Posterior Mean	Posterior 95% CrI	Prior Distribution	Source
Transmission probability per effective contact per day				
Community	0.19	(0.18–0.21)	<i>Uniform</i> (0.10, 0.30)	Calibrated
Household	0.22	(0.16–0.29)	<i>Uniform</i> (0.15, 0.40)	Calibrated
Effectiveness of NPI as a proportional reduction in effective contacts				
(2020/03/25 to 2020/04/21)	0.55	(0.45–0.65)	<i>Uniform</i> (0.25, 0.75)	Calibrated
(2020/04/21 to 2020/05/23)	0.45	(0.38–0.52)	<i>Uniform</i> (0.25, 0.75)	Calibrated
(2020/05/23 to 2020/08/22)	0.45	(0.40–0.50)	<i>Uniform</i> (0.25, 0.75)	Calibrated
(2020/08/22 to 2020/10/31)	0.49	(0.45–0.53)	<i>Uniform</i> (0.25, 0.75)	Calibrated
(2020/10/31 to 2020/12/07)	0.59	(0.51–0.68)	<i>Uniform</i> (0.25, 0.75)	Calibrated
Time-varying daily detection rate generalized logit parameters				
Initial daily rate	0.10	(0.07–0.12)	<i>Uniform</i> (0.005, 0.12)	Calibrated
Final daily rate	0.16	(0.08–0.24)	<i>Uniform</i> (0.005, 0.25)	Calibrated
Rate of change between the initial and final detection rates	0.76	(0.54–0.97)	<i>Uniform</i> (0.01, 1.00)	Calibrated
Time of the sigmoid's midpoint	87.20	(75.60–99.21)	<i>Uniform</i> (30, 100)	Calibrated
Hospitalization Parameters				
Parameter	Mean	95% CI	Source	
Proportion of detected cases being hospitalized				
March 31	0.53	(0.29–0.76)	b	
April 30	0.44	(0.21–0.67)	b	
June 30	0.28	(0.10–0.52)	b	
October 31	0.17	(0.04–0.38)	b	
December 7	0.15	(0.03–0.35)	b	
Proportion of hospitalizations requiring a bed with ventilator ^a				
March 31	0.34	(0.29–0.40)	b	
April 30	0.26	(0.21–0.31)	b	
June 30	0.22	(0.17–0.28)	b	
October 31	0.24	(0.19–0.29)	b	
December 7	0.23	(0.18–0.29)	b	
	Mean	SD	Source	
Length of stay (days) ^a				
All patients	13.45	8.77	Calibrated	
Patients using ventilators	13.88	14.29	Calibrated	
Case Fatality Parameters				
Parameter	Mean	95% CI	Source	
Probability of detected cases dying (%) ^a				
March 31	17.3	(16.1–18.6)	b	
April 30	20.5	(19.9–21.1)	b	
June 30	10.5	(10.1–10.8)	b	
October 31	5.2	(5.0–5.4)	b	
December 7	4.7	(4.5–4.9)	b	
Parameter	Mean	SD	Source	
Time from detection to death in days ^a	8.6	8.6	b	

CI, confidence interval; CrI, credible interval; NPI, non-pharmaceutical intervention; SD, standard deviation.

^aThese values were calculated only using the data of confirmed cases.

^bAuthors' calculation.

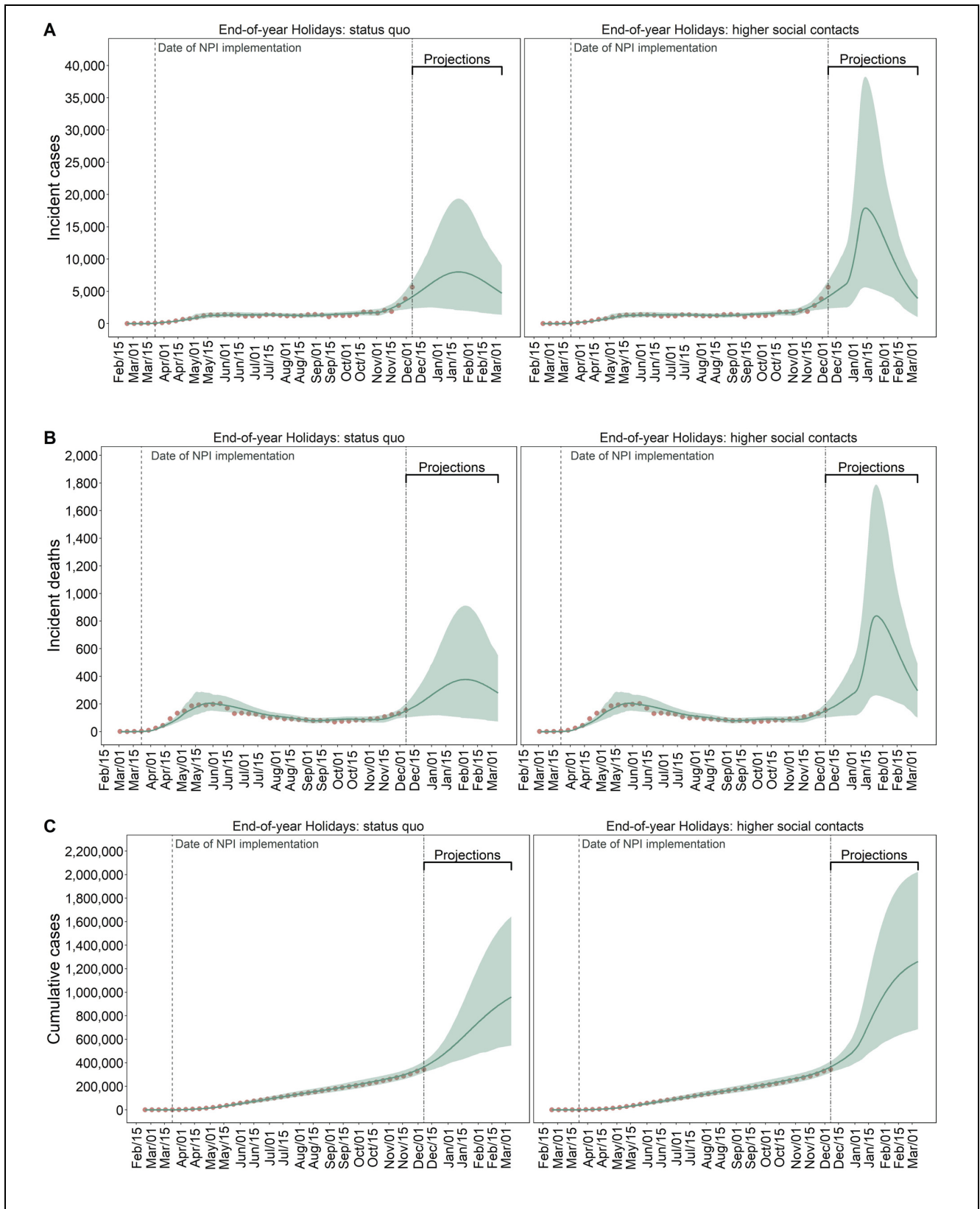


Figure 1 (continued)

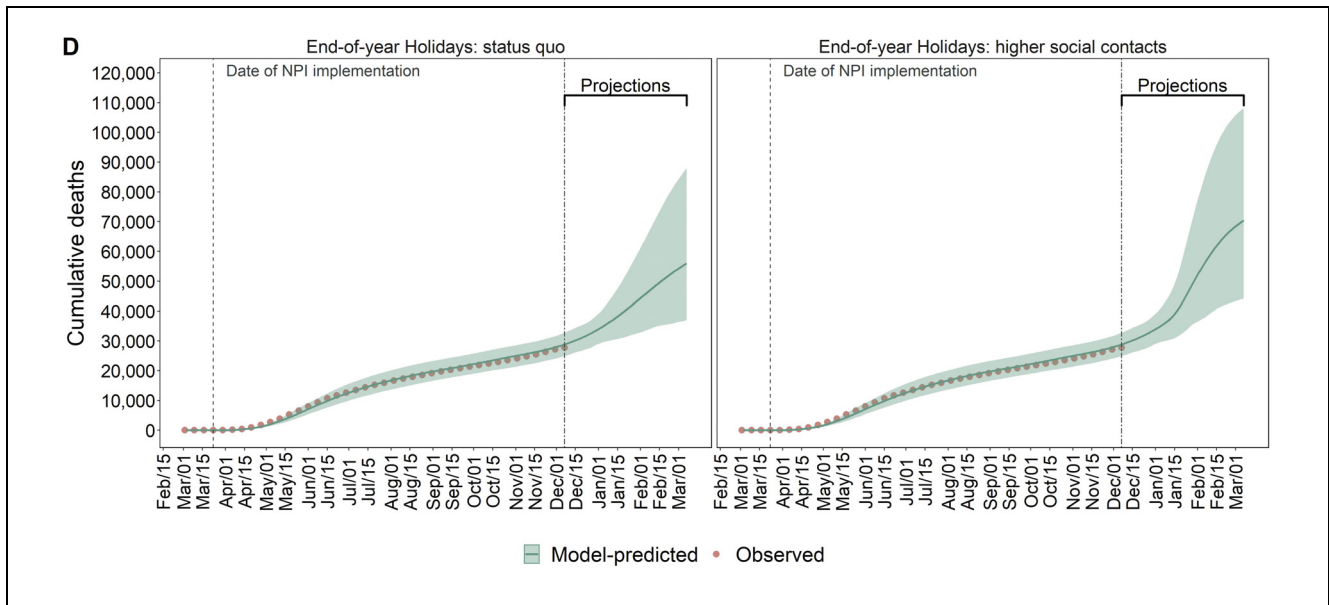


Figure 1 Observed (red dots) and model-predicted (green lines) COVID-19 incident detected cases (A), deaths (B), cumulative cases (C), and deaths (D) in MCMA between February 24, 2020, and March 7, 2021. Left column plots assume compliance with physical distancing during the end-of-year holiday period. Right column plots assume substantially less compliance with physical distancing during the end-of-year holiday period. The double-dashed vertical line represents the last day used for calibration. The green shaded area shows the 95% posterior model-predictive interval of the outcomes, and the green lines show the posterior model-predicted mean based on 1,000 simulations using samples from the posterior distribution.

hospitalizations followed the same general pattern. By December 7, 2020, MCMA had experienced 344,028 confirmed COVID-19 cases and 28,077 deaths (Table 1), which represent cumulative incident and mortality rates of 1,568 and 128 per 100,000 population, respectively. Among confirmed cases, 68,225 (20%) involved hospitalizations and 12,458 (18%) involved ventilator hospitalizations. Patients died in 29% of non-ventilator hospitalizations and 80% of ventilator hospitalizations. The average length of stay in all hospitalized patients was 13.45 days (standard deviation [SD] of 8.77); the average length of stay in ventilator hospitalizations was 13.88 days (SD of 14.29), which represents the time to discharge or death.

On March 17, 2020, we estimated an R_e for COVID-19 in MCMA of 2.15 (95% PI: 2.07–2.25) and decreased to 1.85 (1.81–1.90) immediately after implementation of NPIs and was 1.10 (1.01–1.20) by December 7, 2020 (Supplementary Figure S4). This implies that given the estimated R_e in the early phases of the epidemic and if prepandemic contact patterns had not changed early on, MCMA would have experienced a bigger COVID-19 epidemic than that observed.

Effective contact rates substantially decreased after MCMA's NPIs were initially implemented. Specifically, the calibrated model estimated that effective contacts were 55% (95% PI: 45–65) lower than prepandemic levels in late March 2020 (Table 2 and Supplementary Figures S2 and S3) and 59% lower (51–58) in early December. Our model estimated that 7% (5–11) of the MCMA population—representing 1.5 million people (1.1–2.4)—had previously been infected with SARS-CoV-2 by December 7, 2020 (see Supplementary Figure S5), 24% (14–30) of whom were detected as cases (see Supplementary Figure S6).

Contact Patterns and Epidemic Risks During the End-of-Year Holidays

The trajectory of MCMA's epidemic from late December through mid-January 2021 depends heavily on the extent to which gatherings that traditionally take place in Mexico during the end-of-year holidays occur and cause effective contact rates to rise. Our base case assumption of increased contacts during the holidays projects a peak of 17,904 (95% PI: 5,623–38,271) daily incident cases and

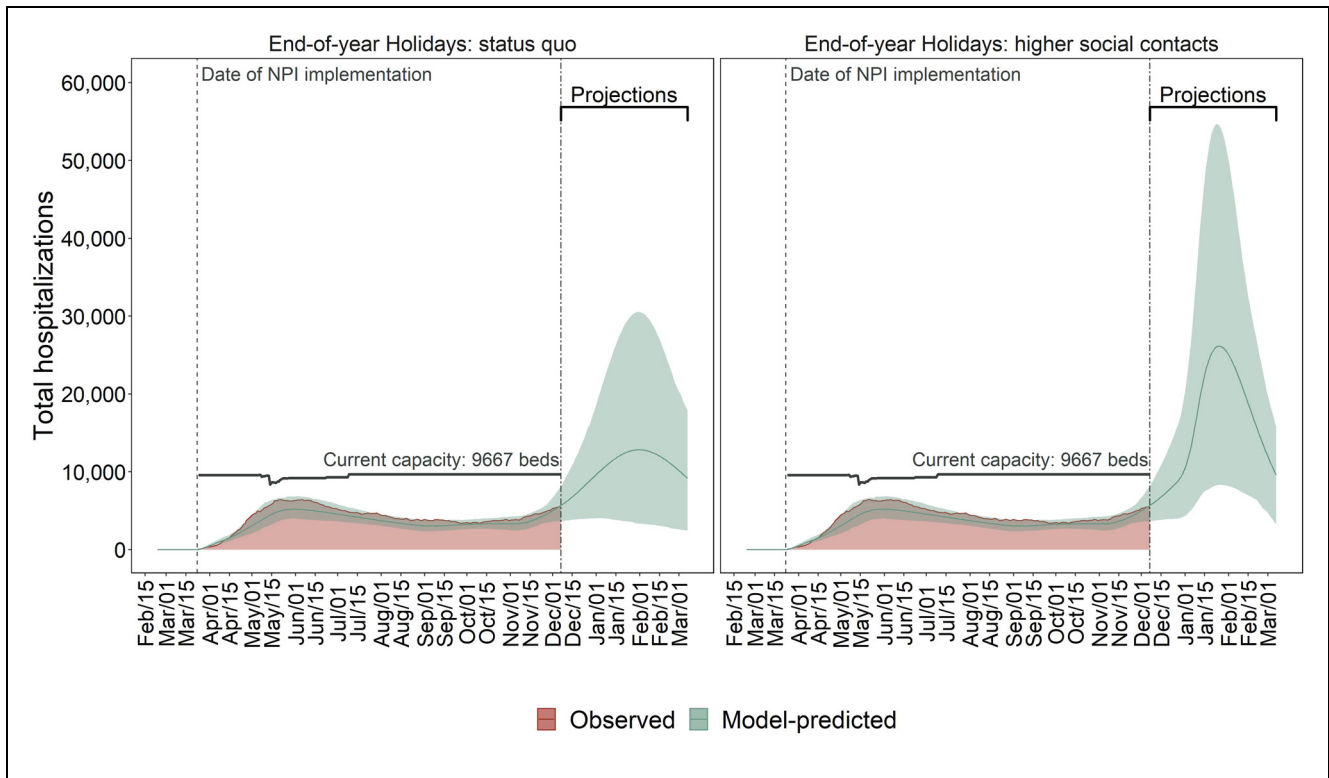


Figure 2 Observed (red area) and model-predicted (green lines) total hospital occupancy and demand in MCMA between February 24, 2020, and March 7, 2021. The left plot assumes compliance with physical distancing during the end-of-year holiday period. The right plot assumes substantially less compliance with physical distancing during the end-of-year holiday period. The double-dashed vertical line represents the last day used for calibration. The green shaded area shows the 95% posterior model-predictive interval of the outcomes, and the colored lines show the posterior model-predicted mean based on 1,000 simulations using samples from the posterior distribution. The horizontal black lines show total COVID-19-specific hospital capacity.

838 (263–1,788) deaths in mid-January 2021 (Figure 1). However, if compliance with physical distancing reduces contacts compared with previous years in this holiday period, the model estimated that daily incident cases and deaths could have a lower peak at 8,011 (2,063–19,365) and 378 (98–912), respectively, occurring in early-February 2021 (Figure 1).

Demand for hospitalization is likely to exceed COVID-19-specific hospital capacity by early 2021, even if end-of-year holiday contacts are reduced. However, these contacts will strongly determine the extent to which capacity is exceeded and the duration of exceedance. Peak demand on January 25, 2021, is projected to be 26,151 (8,318–54,558) with high levels of holiday contacts and 12,830 (3,373–30,538) on January 31, 2021, if holiday contacts are reduced (Figure 2); both far exceed MCMA’s current capacity of 9,667 hospital beds. The probability of exceeding hospital capacity by these dates

is 97% with high levels of holiday contacts versus 64% with low levels of contacts (Figure 5).

Policy Analysis Without Physical Distancing Compliance During the 2020 End-of-Year Holiday Period

NPI policies and compliance from mid-January through early March 2021 will play important roles in mitigating adverse health outcomes and the speed and extent to which hospitalization demand exceeds capacity. The following policy comparisons assume that with less compliance with NPIs, holiday contacts are only 11% (95% PI: 2–19) lower than pre-pandemic levels.

Physical Distancing: Status Quo; Schooling: Not In-Person. Assuming mid-December levels of contacts

resume after the holidays and in-person schools remained closed (i.e., the status-quo), we estimate the following for March 7, 2021: 3,918 (95% PI: 1,033–6,746) incident daily cases and 296 (101–491) incident daily deaths (Figure 3); R_e of 0.82 (0.72–0.91), indicating a declining but still substantial epidemic (Supplementary Figure S4); hospital demand of 9,587 (3,350–15,792) (Figure 4); and a 50% probability of exceeding COVID-19-specific capacity (Figure 5).

Physical Distancing: Increased Compared to Status Quo; Schooling: Not In-Person. However, if on January 10, 2021, physical distancing was intensified relative to December 7 levels resulting in contacts being 57% (95% PI: 53–62) lower than pre-pandemic levels, and in-person schools remained closed, these outcomes would be substantially better. By March 7, we estimate 713 (117–1,547) incident daily cases and 70 (18–124) incident daily deaths (Figure 3); R_e of 0.73 (0.61–0.83) (Supplementary Figure S4); hospital demand at 2,381 (771–4,104; Figure 4), with a <1% probability of exceeding capacity (Figure 5).

In-Person School Reopening in Early 2021

Reopening in-person schooling is a high priority, given the negative societal impacts of these closures. However, epidemic outcomes depend on how reopening is implemented and how much physical distancing can be achieved in schools and other community venues.

Physical Distancing: Status Quo; Schooling: In-Person. Resumption of in-person schooling without reductions in contacts would result in appreciably greater epidemic growth. By March 7, our model estimates that incident daily cases and deaths would be 6,950 (1,829–12,391) and 500 (170–817), respectively (Figure 3); R_e would be 0.83 (95% PI: 0.72–0.94; Supplementary Figure S4); and hospital demand would be 16,034 (5,645–25,891), with the probability of exceeding capacity at 86% (Figures 4 and 5).

Physical Distancing: Increased Compared to Status Quo; Schooling: In-Person. However, if in-person school resumes with contacts reduced substantially below mid-December levels in both schools and the community, then epidemic and hospitalization outcomes would be slightly better than the status quo without school reopening. By March 7, our model estimates that incident daily cases and deaths would be 1,878 (95% PI: 352–3,730)

and 155 (42–271), respectively (Figure 3); R_e would be 0.78 (95% PI: 0.67–0.89; Supplementary Figure S4); hospitalization demand would be 5,096 (1,618–8,781), with the probability of exceeding capacity at 1.1% (Figures 4 and 5).

Policy Analysis With Physical Distancing Compliance During the 2020 End-of-Year Holiday Period

The policy comparisons under a scenario that assumes there are not high end-of-year holiday contacts are consistent with those presented above for the base case. While our primary health and hospital outcomes are generally less extreme due to lower transmission between December 24, 2020, and January 6, 2021, the rank ordering of policies by efficacy does not change (Figures 1–5 and Supplementary Figures S4 and S7). Importantly, if physical distancing compliance were achieved during the end-of-year holiday period, in-person school reopening with appropriate physical distancing would be feasible in mid-January 2021 without sparking substantial additional epidemic growth, although hospitalization capacity would be exceeded. Notably, the scenarios in which COVID-19-specific hospital capacity has a low probability of being exceeded is under increased community physical distancing.

Sensitivity Analysis: Lower Transmission and Severe Disease Risks for Children

When we recalibrated the model assuming that children face lower transmissibility, risk of hospitalization, and mortality than adults, calibrated risks for adults rose to compensate so that overall case rates and hospitalization and death rates matched those reported for MCMA. Hence, projections of the expected cumulative cases and deaths under all scenarios were marginally higher than assuming no differential transmission and severe disease risks for children (Supplementary Figures S8 and S10). Also, in this scenario, hospital exceedance occurs earlier and with a higher probability than in the base case (Supplementary Figures S9, S11, S12, S19, and S20). As noted, these increases relative to the base case were small and did not alter the main conclusions.

Discussion

For MCMA's population of 20 million people, we estimated the epidemic and hospital system effects of resuming in-person schooling in early 2021 and how these

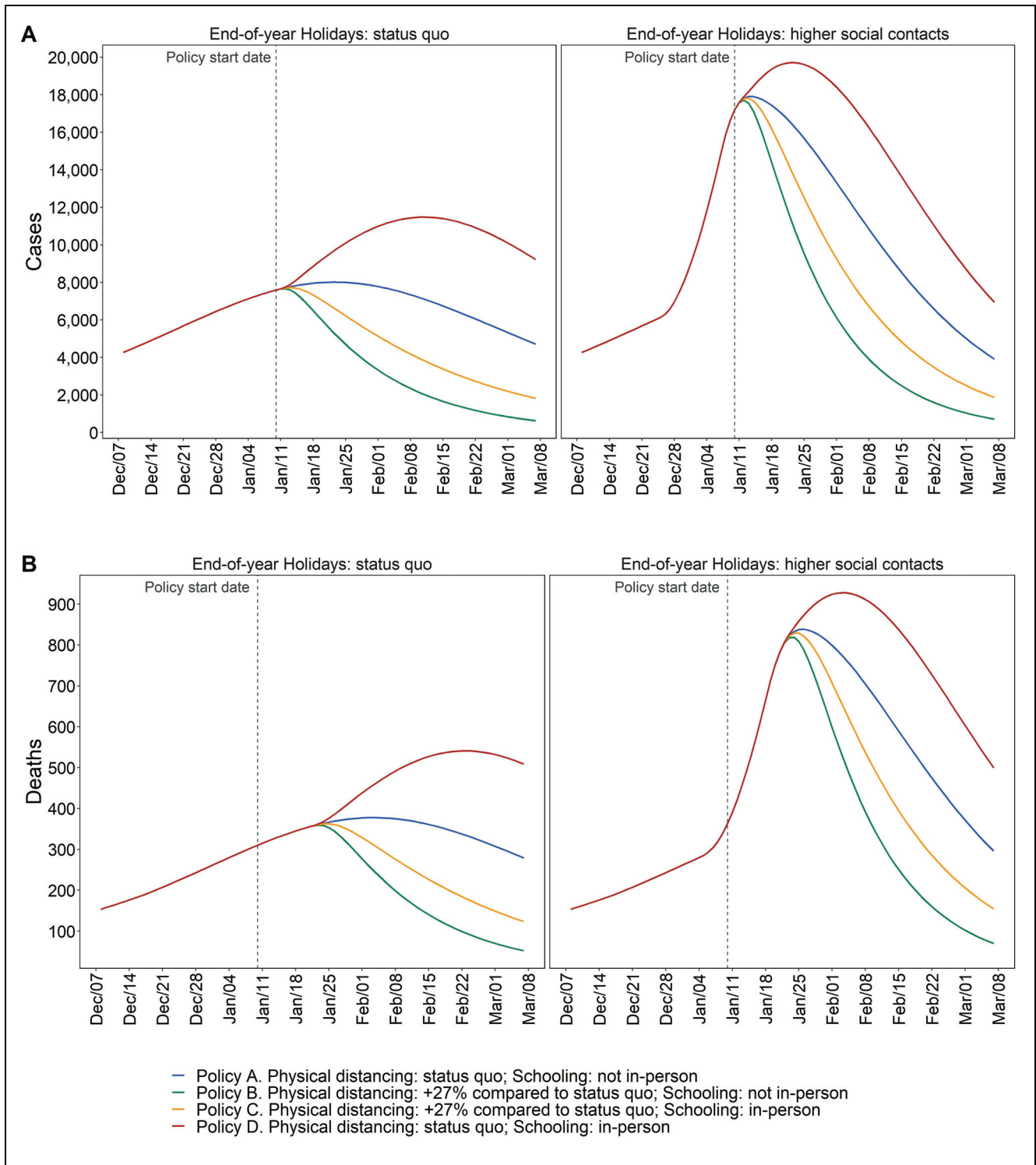


Figure 3 Estimated model-predicted daily incident cases (A) and deaths (B) by scenario in MCMA between December 7, 2020, and March 7, 2021. Left column plots assume compliance with physical distancing during the end-of-year holiday period. Right column plots assume substantially less compliance with physical distancing during the end-of-year holiday period. The vertical dashed line represents the day of policy implementations.

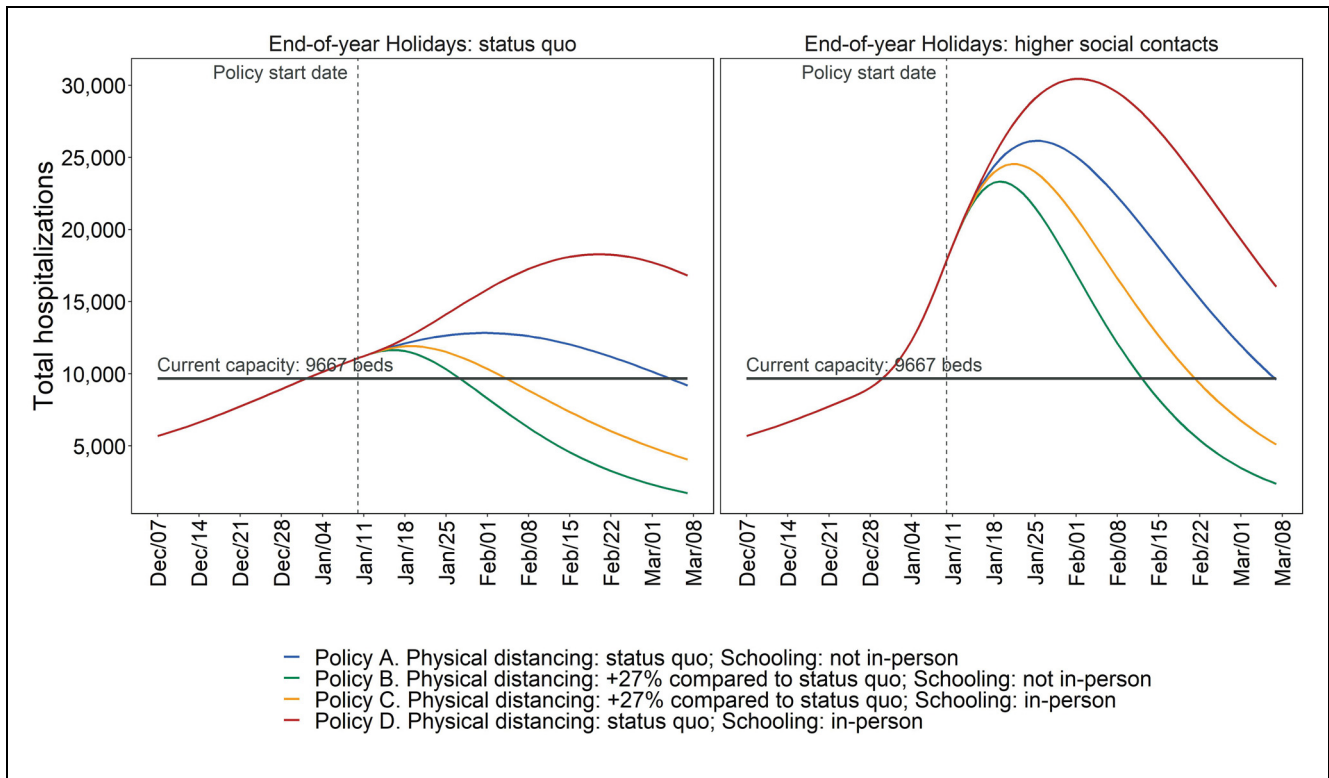


Figure 4 Estimated model-predicted daily hospitalization demand in MCMA between December 7, 2020, and March 7, 2021. The left column plots assume compliance with physical distancing during the end-of-year holiday period. The right column plots assume substantially less compliance with physical distancing during the end-of-year holiday period.

effects depend on the level of end-of-year holiday contacts. Regardless of the level of physical distancing that MCMA residents can achieve during the holidays, hospital demand is highly likely to exceed current capacity unless resources are quickly expanded. We found that high levels of end-of-year holiday contacts greatly exacerbate cases and deaths, with lasting effects through early March 2021, and that these effects could be substantially attenuated by greater physical distancing during the end-of-year holiday period. Without improved physical distancing during the holidays, reopening in-person schools, even with augmented physical distancing, results in appreciable epidemic growth. Thus, we conclude that the feasibility of reopening in-person schooling in the new year depends on reducing mixing and social contacts during the holidays.

While we find that MCMA is expected to exceed hospital capacity as cases continue to rise across scenarios and policies, the timing and magnitude of exceedance differ by scenario. Nonetheless, to meet the surge in hospital demand expected even under optimistic scenarios,

MCMA may have to increase COVID-19-specific capacity by at least 2,000 beds.

Reopening in-person schooling is a high priority. Our findings suggest that provided physical distancing can be maintained both at schools and in the community, reopening may be possible without substantial additional impact on epidemic and health system outcomes. However, if physical distancing cannot be complied with or enforced, school reopening could increase confirmed cases by 376,000 compared with reopening with increased physical distancing. Furthermore, we found that the extent of transmission during the end-of-year policies has an important effect on the feasibility of reopening schools without sparking additional epidemic growth, which is consistent with other findings.²⁶

Our results are in line with previous modeling studies of NPIs in general and compliance with physical distancing in particular.^{3,25,27} Briefly, strengthening both has tremendous potential to reduce epidemic transmission, as does the closure of in-person schooling. But these policies can be highly disruptive, trigger other economic and

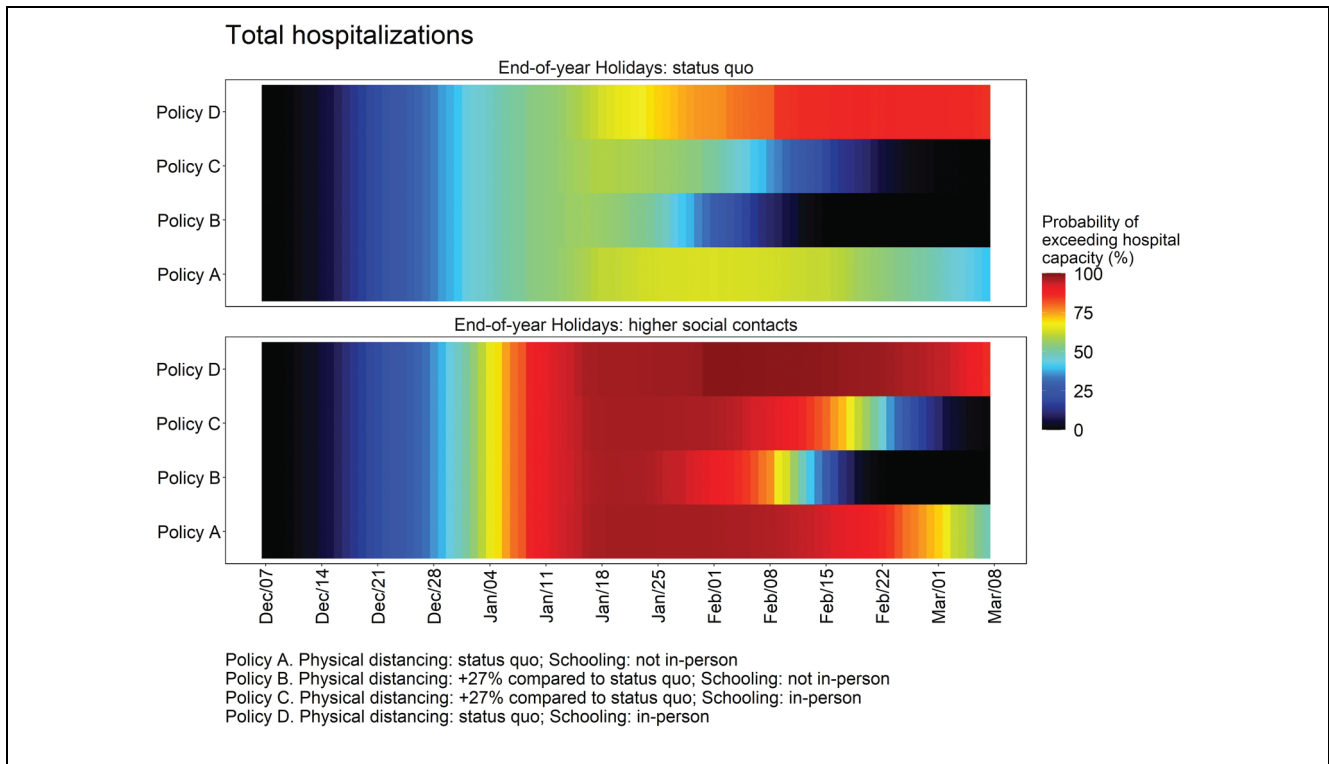


Figure 5 Daily estimated probability of hospitalization demand exceeding COVID-19-specific capacity in MCMA between December 7, 2020, and March 7, 2021, by levels of compliance with physical distancing during the end-of-year holiday period. The top panel assumes compliance with physical distancing during the end-of-year holiday period. The bottom panel assumes substantially less compliance with physical distancing during the end-of-year holiday period.

social costs, and are increasingly provoking backlashes among frustrated and weary communities throughout the world. Our findings underscore a theme evident in similar studies: policy decisions about reopening various venues and institutions are interrelated in their effects. They must be considered as part of the tradeoffs that include health, economic, and social outcomes.

Our analysis has several limitations. First, while our model is stratified by age to account for differential mixing, the base-case analysis does not include differential transmission by younger people.²⁴ Some studies find that younger children may transmit less and have differentially lower mortality and hospitalization risks than teens and adults.^{24,25} If children are differentially less likely to transmit then, at least for primary schools, our results may underestimate the possibility of resuming in-person schooling with physical distancing without exacerbating the epidemic and could be viewed as conservative. However, our findings are qualitatively similar when allowing differential transmission and severe disease risks in children in a sensitivity analysis. Second, our analysis

does not account for vaccination. However, the periods we focus on precede plausible mass vaccination, given current expectations regarding vaccine roll-out in Mexico.²⁸ Findings from our analysis will be useful inputs for a more comprehensive economic evaluation of policy alternatives in future research.

Our study has several strengths. First, we use the SC-COSMO model, a dynamic transmission model that accounts for realistic contact patterns based on adjusted population density²⁹ and community and household transmission.¹¹ The SC-COSMO framework enables quantification and propagation of uncertainty to generate probabilistic projections—not only producing estimates of expected outcomes but also allowing assessment of the probability and magnitude of extreme events like exceeding hospital capacity under different scenarios.³⁰ We use comprehensive data on cases, deaths, and hospitalizations to estimate the model's parameters, allowing us to accurately represent the epidemic dynamics in MCMA. Additionally, we have information on current hospital capacity in the city that allows us to determine

when and how likely it is to exceed COVID-19-specific hospital capacity under different scenarios.


As MCMA's COVID-19 epidemic continues to evolve, there is a high probability that the area's hospital capacity will be outstripped by early January 2021, especially if contacts during the end-of-year holidays cannot be substantially reduced. As resumption of in-person school is a major priority, it is crucial to ensure that NPI measures are instituted in schools. The unavoidable increases in contacts that school reopening will trigger are offset by more effective physical distancing in the community. Even if schools are not reopened, and physical distancing in the community improves, there is an urgent need for MCMA to increase its hospital capacity. Finally, our findings highlight the importance of simulation modeling-based policy analysis as a tool to support timely decision making.


Acknowledgments

The authors are grateful for feedback received for development and model use during the COVID-19 epidemic from researchers, policymakers, and stakeholders.

ORCID iDs

Fernando Alarid-Escudero  <https://orcid.org/0000-0001-5076-1172>

Andrea Luviano  <https://orcid.org/0000-0002-2624-4850>

Anneke L. Claypool  <https://orcid.org/0000-0002-2280-2296>

Supplemental Material

Supplemental material for this article is available on the *Medical Decision Making Policy & Practice* website at <https://journals.sagepub.com/home/mpp>.

References

- World Health Organization. WHO coronavirus (COVID-19) dashboard. Available from: <https://covid19.who.int>
- Sosa-Rubí SG, Seiglie JA, Chivardi C, et al. Incremental risk of developing severe COVID-19 among Mexican patients with diabetes attributed to social and health care access disadvantages. *Diabetes Care*. 2021;44(2):373–80. doi:10.2337/dc20-2192
- Zhang Z, Yao W, Wang Y, Long C, Fu X. Wuhan and Hubei COVID-19 mortality analysis reveals the critical role of timely supply of medical resources. *J Infect*. 2020;81(1):147–78.
- Robert R, Reignier J, Tournoux-Facon C, et al. Refusal of intensive care unit admission due to a full unit: impact on mortality. *Am J Respir Crit Care Med*. 2012;185(10):1081–7.
- Ritchie H, Mathieu E, Rodés-Guirao L, et al. Coronavirus pandemic (COVID-19). Available from: <https://ourworldindata.org/coronavirus>
- Dirección General de Epidemiología. Datos Abiertos Dirección General de Epidemiología. Available from: <https://www.gob.mx/salud/documentos/datos-abiertos-152127>
- Hasell J, Mathieu E, Beltekian D, et al. A cross-country database of COVID-19 testing. *Sci Data*. 2020;7(1):345.
- Choi W, Shim E. Optimal strategies for vaccination and social distancing in a game-theoretic epidemiologic model. *J Theor Biol*. 2020;505:110422.
- Instituto Nacional de Estadística y Geografía. Encuesta Nacional sobre Disponibilidad y Uso de Tecnologías de la Información en los Hogares (ENDUTIH) 2019. Available from: <https://www.inegi.org.mx/programas/dutih/2019/>
- Morales A. Pide AMLO a la población no salir durante 10 días por COVID-19. Available from: <https://www.eluniverso.com/salud/2020/04/10/pide-amlo-la-poblacion-no-salir-durante-10-dias-por-covid-19>
- Alarid-Escudero F, Luviano A, Kunst N, Peralta Y, Goldhaber-Fiebert JD. Accounting for household transmission dynamics in realistic epidemic models. In: 42nd Annual Meeting of the Society for Medical Decision Making; October 18, 2020; Chicago, IL.
- Jalal H, Pechlivanoglou P, Krijkamp E, Alarid-Escudero F, Enns E, Hunink M. An overview of R in health decision sciences. *Med Decis Making*. 2017;37(7):735–46.
- Wallinga J, Teunis P. Different epidemic curves for severe acute respiratory syndrome reveal similar impacts of control measures. *Am J Epidemiol*. 2004;160(6):509–16.
- Consejo Nacional de Población (CONAPO). Estimaciones y proyecciones de la población por entidad federativa. Datos de proyecciones. Available from: <https://datos.gob.mx/busca/dataset/proyecciones-de-la-poblacion-de-mexico-y-de-las-entidades-federativas-2016-2050>
- Agencia Digital de Innovación Pública. Agencia Digital de Innovación Pública. Available from: <https://adip.cdmx.gob.mx>
- Lauer SA, Grantz KH, Bi Q, et al. The incubation period of coronavirus disease 2019 (COVID-19) from publicly reported confirmed cases: estimation and application. *Ann Intern Med*. 2020;172(9):577–82.
- He X, Lau EHY, Wu P, et al. Temporal dynamics in viral shedding and transmissibility of COVID-19. *Nat Med*. 2020;26(5):672–5. doi:10.1038/s41591-020-0869-5
- Ashcroft P, Huisman JS, Lehinen S, et al. COVID-19 infectivity profile correction. *Swiss Med Wkly*. 2020;150:w20336. doi:10.4414/sm.w.2020.20336.
- Lloyd-Smith JO, Schreiber SJ, Kopp PE, Getz WM. Super-spreading and the effect of individual variation on disease emergence. *Nature*. 2005;438(7066):355–9.
- Raftery AE, Bao L. Estimating and projecting trends in HIV/AIDS generalized epidemics using incremental mixture importance sampling. *Biometrics*. 2010;66(4):1162–73.
- Ryckman T, Luby S, Owens DK, Bendavid E, Goldhaber-Fiebert JD. Methods for model calibration under high

- uncertainty: modeling cholera in Bangladesh. *Med Decis Making*. 2020;40(5):693–709.
22. Sawaya GF, Sanstead E, Alarid-Escudero F, et al. Estimated quality of life and economic outcomes associated with 12 cervical cancer screening strategies: a cost-effectiveness analysis. *JAMA Intern Med*. 2019;179(7):867–78.
 23. Davies NG, Klepac P, Liu Y, et al. Age-dependent effects in the transmission and control of COVID-19 epidemics. *Nat Med*. 2020;26(8):1205–11.
 24. Fung HF, Martinez L, Alarid-Escudero F, et al. The household secondary attack rate of SARS-CoV-2: a rapid review. *Clin Infect Dis*. 2020;73(suppl 2):S138–S145.
 25. Ludvigsson JF. Children are unlikely to be the main drivers of the COVID-19 pandemic—a systematic review. *Acta Paediatr*. 2020;109(8):1525–30.
 26. Macartney K, Quinn HE, Pillsbury AJ, et al. Transmission of SARS-CoV-2 in Australian educational settings: a prospective cohort study. *Lancet Child Adolesc Health*. 2020;4(11):807–16.
 27. Roosa K, Lee Y, Luo R, et al. Real-time forecasts of the COVID-19 epidemic in China from February 5th to February 24th, 2020. *Infect Dis Model*. 2020;5:256–63.
 28. Secretaría de Salud de México. Política Nacional de Vacunación Contra el Virus SARS-CoV-2, para la prevención de la Covid-19 en México. Documento rector. Available from: https://coronavirus.gob.mx/wp-content/uploads/2021/04/28Abr2021_13h00_PNVx_COVID_19.pdf
 29. Reitsma M, Alarid-Escudero F, Andrews J, et al. Methods for constructing sub-national contact matrices for transmission models of respiratory viruses like SARS-Cov-2 (COVID-19). *Med Decis Making*. 2021;41(4):E62–E64.
 30. Gurdasani D, Ziauddeen H. On the fallibility of simulation models in informing pandemic responses. *Lancet Glob Health*. 2020;8(6):e776–e777.
 31. Instituto Nacional de Estadística y Geografía. Densidad de población. Available from: <http://www.cuentame.inegi.org.mx/poblacion/densidad.aspx?tema=P>